Bulletin of Business and Economics, 13(1), 736-748
https://bbejournal.com
https://doi.org/10.61506/01.00263

Glaucoma Disease Classification by Using Fundus Images

Allah Rakha[1], Dr. Sohail Masood[2], Arslan Akram[3], Muhammad Faseeh Sultan[4]

Abstract

Optic Disc (OD) and Optic Cup (OC) damage is caused by the eye condition glaucoma. OD is the morphological structure that is apparent in the cross-sectional view of the optic nerve connecting to the retina, while OC is the core region of OD. The morphological changes in the optic disc (OD) and optic cup (OC) often happen before visual field issues when glaucoma begins. Optic nerve head damage caused by glaucoma is permanent. Glaucoma is the greatest global cause of irreversible blindness, according to data from the World Health Organization (WHO). Only 10 to 50 percent of glaucoma patients, according to population-level surveys, are aware that they have the condition. As a result, glaucoma early identification is crucial for preventing irreversible eye damage. Glaucoma is a vision disorder that frequently affects older people and renders them permanently blind. Glaucoma affects 2.5% of people of all ages and 4.8% of people over the age of 75. Using MobileNetV2, this study suggests a unique deep transfer learning model for categorizing glaucoma. With regard to the error, with the least amount of expense, MobileNetV2 is a framework that optimizes memory consumption and execution speed. To increase the dataset and MobileNetV2's precision, data augmentation techniques were used. Using the HRF dataset, the suggested deep learning model's effectiveness is assessed. Results from the suggested procedure are accurate to 98%. Medical professionals can find the optimum course of treatment for their patients with the help of automated glaucoma classification.

Keywords: Glaucoma, World Health Organization (WHO), MobileNetV2, Optic disk (OD) and optic cup (OC)

1. Introduction

1.1. Introduction of the Study

Medical imaging is a technique used to create images of the human body for use in disease diagnosis and assessment. The process is supposed to select the approaches that noninvasively create images of the internal part of the body. Nowadays, digital images of the body are attained to automate the diagnostic procedure in medical imaging. Figure 1.1 shows various digital images (i.e., retinal image, brain MRI sample, X-rays, and dermoscopic sample) which are being employed for CAD of different medical diseases (Singh et al., 2023) . The retinal images are acquired using the fundus camera, which is the first step towards the CAD-based diagnostic, treatment, monitoring, and surgery planning of various eye diseases. Retinal imaging allows the ophthalmologist to see the patient's eye more closely and precisely, which makes them able to observe early signs of eye diseases. Retinal imaging is used in ophthalmic diagnostics to diagnose eye issues caused on by diabetes, including diabetic retinopathy, diabetic macular edema, and glaucoma. In the screening process, extensive usage of retinal imaging increases the need of processing the large volume of samples. ((Nguyen et al., 2022) (Gharahkhani et al., 2020) (Robbins et al., 2021) (Khatib & Martin, 2020)).

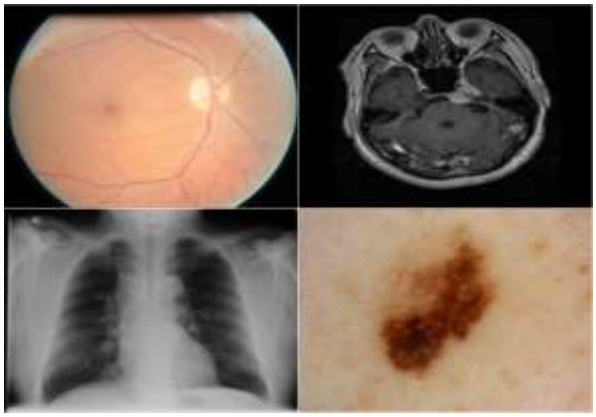

Figure 1: Images used for the diagnosis of different

1.2. Understand the Eye to Understand Glaucoma

The majority of the eye's outer surface is covered by the sclera, a thick, white coating. The conjunctiva, a translucent, thin layer, covers the sclera. The pupil and iris are concealed behind the cornea, a transparent area that resembles a window at the front of the eye. The eye's colored iris, which is a muscle, moves in and out to admit light into the eye. The clear cornea shields the pupil, or hole where light enters the eye, which is situated in the center of the iris. Our eye's lens directs this light onto the retina, which is

[1] Faculty of Computing, Department of Computer Science and Information Technology, The Superior University, Lahore, 54000, Pakistan
[2] Faculty of Computing, Department of Computer Science and Information Technology, The Superior University, Lahore, 54000, Pakistan
[3] Faculty of Computing, Department of Computer Science and Information Technology, The Superior University, Lahore, 54000, Pakistan, MLC Lab, Okara, 56310, Punjab, Pakistan
[4] Faculty of Computing, Department of Computer Science and Information Technology, The Superior University, Lahore, 54000, Pakistan

found at the back of the eye. The retina converts light pictures into electrical impulses that are subsequently transferred to the brain via the optic nerve via the nerve cells and fibers of the retina. The optic disc is the region of the retina where the optic nerve connects to the remaining retina to leave the eye and proceed to the brain. [https://glaucoma.org/eye-anatomy]

1.3. A Healthy Eye

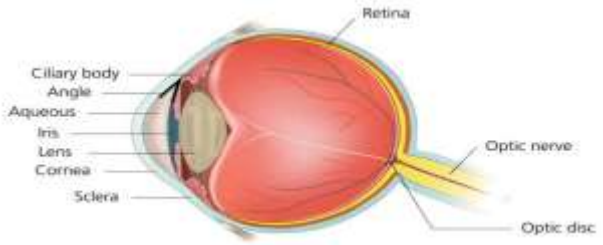

Figure 2: Eye-anatomy

1.4. Healthy Eye Drainage

The ciliary body creates aqueous humor, the clear liquid that fills the front of the eye.

The pupil is where the fluid exits. After there, it enters the drainage system of the eye's trabecular meshwork and network of canals. The balance between the volume of fluid produced and the volume that drains out of the eye determines the intraocular pressure, or "IOP," of the eye. Your eye's fluid system will produce the necessary amount of fluid if it's working properly. Similarly, if the drainage mechanism in your eye is functioning properly, fluid can flow freely out to minimize pressure building. The health of the eye depends on proper drainage, which is an active, ongoing process that helps maintain eye pressure at a normal level.

1.5. Glaucoma

Diabetes is a condition marked by elevated blood sugar levels. Several eye conditions, including glaucoma, diabetic retinopathy (DR), and diabetic macular edema (DME), can leave victims with partial or complete vision loss. Optic disc (OD) and optic cup damage is caused by the eye condition glaucoma. The cross-sectional view of the optic nerve leading to the retina shows the morphological structure known as OD and the central component of OD is known as OC. (Nawaz et al., 2022) When glaucoma develops, the morphological alterations in the optic cup (OC) and optic disc (OD) typically occur before visual field problems. Changes in the OD/parameters OC's may therefore be an indication of optic nerve damage (Zhao et al., 2021) The optic nerve is harmed by glaucoma, popularly known as "the sneak thief of sight," which results in enduring vision impairment. Glaucoma damages the head of the optic nerve in an irreversible manner.

Fig 3: https://www.richieeyeclinic.com/surgery-cenk4ter/glaucoma-testing-treatment/

Digital fundus imaging, optical coherence tomography, visual field testing, and fundoscopy are only a few of the clinical techniques utilized to detect the optic nerve head injury in glaucoma (Devecioglu et al., 2021). Because of the usual intraocular pressure (IOP)) in the eye, glaucoma is an evil eye condition that damages the eye's optic nerve (Nawaz et al., 2022).

According to the World Health Organization (WHO), glaucoma is the leading global cause of irreversible blindness (Devecioglu et al., 2021). By the year 2040, there will be around 112 million individuals living with glaucoma. However, because there are no early indications, many people are unaware of this predicament. The most prevalent type of chronic glaucoma arises from a loss of fluid-draining ability in the trabecular meshwork of the eye. Consequently, as the pressure inside the eyes rises, the optic nerve is harmed. Glaucoma treatment is essential for preserving vision and quality of life because glaucoma is a chronic neurological condition that can only be managed. Because glaucoma is an asymptomatic ailment, patients frequently don't seek medical attention

until it's too late to avert blindness. Only 10% to 50% of glaucoma patients, according to population-level surveys, are aware of their affliction (Neto et al., 2022). Therefore, early glaucoma detection is essential for avoiding permanent eye damage. Glaucoma is a visual disorder that frequently affects older persons and results in lifelong blindness (Kanse & Yadav, 2019). Glaucoma affects 2.5% of people of all ages, while it affects 4.8% of people over 75 (Camara et al., 2022). Additionally, glaucoma risk factors can include eye conditions such trauma, cataracts, tumors, inflammatory processes, and ocular hypertension. The risk factors that affect the likelihood of developing blindness include family history, the course of the disease, the level of eye pressure at disease onset, the age at which the disease first manifests, prior eye conditions and injuries, topical and systemic corticosteroid use, tobacco, alcohol, and drug use, diabetes, lung disease, heart disease, cerebrovascular disease, and high blood pressure (O'bryhim et al., 2022).

1.6. Who Gets Glaucoma

- People of various ages, including infants, adolescents, and younger and older adults, can suffer glaucoma.
- Everyone is susceptible to glaucoma, although some people are more vulnerable than others.

1.7. WHO Are More At Risk Are Those WHO

• Are over 40?
• Are of African or Caribbean origin;
• Are closely related to someone with glaucoma.

If you are over 40 and have a sibling, parent, child, or other relative with glaucoma, the NHS will cover the cost of your eye exam.

1.7.1. Glaucoma Symptoms

Below are early warning signs of glaucoma that should never be ignored. Should you notice any of these symptoms, call our optometry team immediately.

Severe Eye Pain or Nausea- You will notice this symptom because the eye pain associated with glaucoma can become unbearable. There may be redness in the eyes, intense headaches, or even vomiting.

Increased Light Sensitivity- Have you noticed that being around any light source is almost painful for your eyes? Elevated intraocular pressure, referred to as IOP, is often why this happens.

Blurry Eyes- Increased pressure in your eyes can push excess fluid into your cornea. As a result, your eyes may be cloudy or even look like they are waterlogged.

Halos around Lights- Halos are bright colored circles that appear around any light source. If you notice these, you could have the beginning symptoms of
glaucoma. [https://www.eyecareassociates.com/blog/549383-early-symptoms-of-glaucoma]

1.7.2. Diagnosis of Glaucoma

Ophthalmologists can conduct visual field tests to determine whether a patient has glaucoma, and significant symptoms of the condition, such as deformations of the optic disc, parapapillary atrophy, or defects in the retinal nerve fiber layer, can be directly seen using color retinography, a retinal imaging technique that is widely used. The distortion of the optic disc has been the one of these symptoms that has received the most research for glaucoma early diagnosis. The segmentation of the optic disc and cup is the most popular method for the automated diagnosis of glaucoma, and the vertical Cup-to-Disc Ratio (CDR) has received substantial study as a method for determining the progression of glaucoma (Hervella et al., 2022). A glaucoma patient's CDR value is disproportionately higher than the average value. Many CDR-based segmentation approaches for glaucoma screening have been proposed during the past few decades. These CDR-based approaches have low sensitivity issues and rely heavily on segmentation accuracy while ignoring other metrics. These CDR-based approaches have low sensitivity issues and rely heavily on segmentation accuracy while ignoring other metrics (Nayak et al., 2021).

Tonometry: A common test for determining the pressure inside the eye is tonometry, sometimes referred to as intraocular pressure (IOP). The normal range of ocular pressure is 12 to 22 mmHg. People who have higher than usual ocular pressure are more prone to develop glaucoma. But glaucoma is not always present when the pressure is higher than normal. In contrast, lower ocular pressures may lead to the development of glaucoma rather than greater pressures (Islam et al., 2021).

Figure 1.4: Checking the eye pressure using tonometry

Ophthalmoscopy: By analyzing the optic nerve's appearance and color, it helps identify glaucoma damage. If the ocular nerve, which transmits visual data from the eyes to the brain, seems irregular or the intraocular pressure (IOP) is outside of the normal range, further testing is required (Islam et al., 2021).

Figure 5: your doctor can see your optic nerve with the aid of an ophthalmoscope.

Visual Field Testing: Perimetry is another term for visual field testing. A diagram of the complete field of view is produced. This examination will help determine whether glaucoma has affected the eyesight or not (Cvenkel & Kolko, 2020)**.**

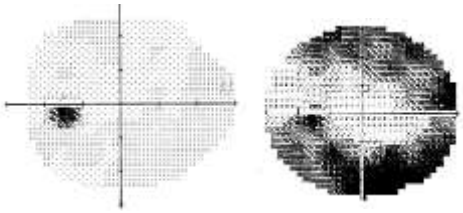

Figure 6: Visual field within normal limits Visual field outside normal limits

Results of tests on a visual field with glaucoma-related vision loss (on the left) and a visual field with normal vision and no vision loss (on the right). Loss of eyesight in a visual field is represented by darker grey and black regions. Since there is no vision in the optic disc, it appears black in both fields; this is typical (https: //glaucoma.org/wp-content/. 2021).

Gonioscopy: Gonioscopy is a method where the cornea's angle with the iris is examined by gently contacting the layer of the eye with a special reflective device .Depending on whether or not this angle is open, the doctor will determine what type of glaucoma is present and how severe the condition is (Islam et al., 2021).

Figure 4: Checking the eye pressure using tonometry

Pachymetry: The cornea's thickness is measured using the Pachymetry technique. When tonometry is performed, the cornea's thickness appears to be a good indicator of how much the cornea may swell (Arbeiter et al., 2021).

Nerve Fiber Analysis: Recent glaucoma screening methods include nerve fiber analysis, which measures the diameter of the nerve fiber surface. Narrower areas might be signs of damage from glaucoma (Ansari et al., 2021).

Computer-aided diagnosis: Computer-aided diagnosis (CAD) is a helpful method for detecting early-stage glaucoma in retinal fundus images. Ophthalmologists will perform better screening processes with the use of a CAD system for glaucoma diagnosis (Latif et al., 2022).

Imaging Technique: The Retinal Imaging technique is critically used for diagnosing retinal diseases. Fundus imaging and optical coherence tomography (OCT) imaging are the two most significant methods of retinal imaging. The diagnosis of glaucoma requires this scan. It is utilized to identify retinal nerve fiber layers around the optic nerve, a key indicator of early glaucoma damage. Fundus Imaging is commonly used in population based large-scale discovery of Glaucoma, Diabetic Retinopathy, and Age-related Macular Degeneration. Fundus Image is also utilized in diagnosing Glaucoma as well as Diabetic Retinopathy. A Fundus camera is a device used specifically for capturing the images of the retina (Alghamdi & Abdel-Mottaleb, 2021).

Figure 8: Fundus Camera

1.8. Background of the Problem

The primary study field that makes use of deep learning DL, computer vision, and image processing is medical imaging, and for the diagnosis of different diseases i.e., brain tumor, skin cancer, lung cancer, and eye diseases, etc. Retinal or Fundus images are utilized for identification of abnormalities of the eye and may be helpful to save the patient's vision. Glaucoma is underdiagnosed since it has no symptoms in the beginning. The prognosis gets worse as glaucoma gets worse. General population screening is rarely seen as cost-effective due to the relatively small numbers of eye health specialists—optometrists and ophthalmologists—and their geographic concentration in affluent urban centres. Conversely, specialized screening is economical. In the literature, CDR is one of the most significant medical indications used to detect the presence of glaucoma. Typically, ophthalmologists use a vertical CDR to identify the cup and disc areas and diagnose glaucoma. But pinpointing the location of the cup is exceedingly challenging. Again, because blood vessels and the tissues surrounding the cup are intertwined, calculating the optic cup boundary automatically is difficult. Early ONH changes are difficult to detect due to the wide range of CDR, and ONH structures differ between ethnic groups. Therefore, it is still crucial to create alternative detection methods to help clinicians identify glaucoma at an early stage. Some research employs the thresholding procedure for the detection of glaucoma based on characteristics. Doctors can use deep learning to diagnose patients more quickly and effectively. In order to prevent a disease, it can predict its risk. Deep learning aids in the analysis of medical data by researchers for disease treatment. However, it can frequently be challenging and time-consuming to analyze medical images. Early detection and treatment of eye diseases provide us a tremendous chance to save people's vision before it is lost.

1.9. Problem Statement

The accuracy of the existing model was needed to be improved. The present research is carried out to resolve the above challenges. Glaucoma is underdiagnosed; its early stages are asymptomatic. As glaucoma progresses, prognosis worsens. Due to the relatively low numbers of eye health professionals—optometrists and ophthalmologist and their geographic concentration in wealthy urban centers, general population screening is rarely considered cost-effective. On the other hand, targeted screening is cost-effective. One of the important medical features used in the literature to find the presence of glaucoma is CDR.

1.9.1. Purpose of the Study

The main objective of this study is to develop a method that can automatically classify and localize anomalies in the chest. The ability to detect these disorders automatically and with high accuracy could significantly improve real-world diagnosis processes.

1.9.2. Research Aims, Methods, Objectives and Research Questions

1.9.3. Research Aims

It is aim of this research to overcome the exciting technique issue, high false- negative rate and robustness. Which algorithm and technique will provide best results/accuracy in term to localize and classify glaucoma disease?

1.9.4. Research Questions

RQ-1: How to identify the models that are performing well in terms of accuracy, sensitivity, recall, specificity, and precision.

RQ-2: How to establish a foundational model that allows for more research using alternative methods.

RQ-3: How to provide an affordable solution that could eventually result in the creation of automatic glaucoma disease diagnosis to lessen the burden on pathologists and ophthalmologists in order to support a broad patient base.

RQ-3: What are the ways to use deep learning to automate the identification of glaucoma.

1.9.5. Research Objectives

- To determine which models are performing well in terms of precision, recall, specificity, sensitivity, and accuracy.
- To create a base model on which more investigation can be performed with other approaches.
- To develop a cost-effective solution that may lead to the development of automatic detection of glaucoma diseases to decrease the workload of the ophthalmologists and pathologists to support a large number of patients.
- Think of possible solutions that could help automate glaucoma detection with deep learning.

2. Literature Review

(Saxena et al., 2020) Introduces a (CNN) convolutional neural network-based deep learning architecture for accurately identifying glaucoma disease. The CNN can be used to distinguish between the patterns created for glaucoma and non-glaucoma. For differentiation, CNN offers a hierarchical structure for the images. The planned work can be evaluated on a total of six levels. To achieve the required performance in the glaucoma detection, the dropout technique is also applied in this instance. The SCES and ORIGA datasets were used in the studies. The analysis is done for both the dataset and the accuracy is 0.822 for the ORIGA dataset and 0.882 for the SCES dataset, respectively.

In order to diagnose glaucoma sequentially, the authors (Guo et al., 2020) suggested a novel automatic glaucoma testing approach that retrieved and analyzed clinically computed and image-based features. The Adaptive Synthetic (ADASYN) algorithm has been used to minimize the imbalance in the ORIGA dataset since the quantity of glaucomatous fundus images is about three times higher than the normal class. The segmentation features for the optic cup and disc are extracted using the CP-FD-UNet++, an upgraded version of the U-Net neural network. The approach used on the freely available ORIGA dataset performed better than other algorithms already in use, with accuracy and AUC of 0.843 and 0.901, respectively.

Canny Edge Detection (CED) is a technique that was developed by (Shoba & Therese, 2020). Then, using morphological approaches, the blood vessels from the suspected sample were segmented. To compute the final feature, a study employing finite element modelling (FEM) was conducted in the subsequent stage. During the support vector machine (SVM) training phase, the computed features handle the classification task. Photographs of the retinal fundus were used by the writers, who obtained them from an eye hospital (glaucoma and healthy image).The classification outcomes demonstrate that the retinal picture was accurately identified as either sick or not. The suggested SVM classification technique yields classification results with 93.22% accuracy, 88.96% specificity, and 84.96% sensitivity. The research holds up well to noisy samples. However, a challenging dataset is required for the model's evaluation. On a small dataset, the model's limitations are examined.

In the same year, another study was carried out by (Ajitha & Judy, 2020) utilizing data from ORIGA and DRASHTI-GS. In this study, the accuracy of VGG16 and ResNet50 are compared. This study divided glaucoma into two categories as a result: glaucoma and no glaucoma. In the DRASHTI-GS dataset, this research suggests that ResNet50 outperforms VGG16 in terms of performance. The accuracy percentage for the ResNet50 model was 92.5%.

In 2020 (Nawaz et al., 2022) provided a technique that combines fuzzy k-means clustering with the Fast Region-based Convolutional Neural Network (FRCNN) algorithm to automatically segment and locate diseases. Since datasets don't typically contain bounding-box annotations, we created them using ground truths. For the FRCNN object detection technique to work, these annotations are necessary. Using FKM clustering to separate the annotated images, the annotated images are then utilised to train the FRCNN for localization. The authors came to their conclusions using datasets from DR-HAGIS, HRF, MESSIDOR, ORIGA, and Diaretdb1. On all datasets, the newly presented framework achieved 95% accuracy. Although the strategy has higher economic expenses, it performs better in terms of glaucoma segmentation.

A study was carried out in 2021 by (Fu'adah et al., 2021). There are two classes in the rim-one database r2: normal and glaucoma. An accuracy of 91% is obtained by using the Convolutional Neural Network (CNN) approach with three hidden layers and 3x3 filters with sizes of 16, 32, and 64. (Serte & Serener, 2021). proposed models for convolutional neural networks. An ensemble of graph-based saliency is created using Alexnet, ResNet-50, and ResNet-152, and three methods are suggested for automatic glaucoma identification.. The suggested method used convolutional neural networks to conduct classification after cropping the optic disc using graph-based saliency. On a public dataset with 1542 retinal pictures, the proposed approach was tested, and its accuracy was 0.88. The classification performance for glaucoma is improved, although this approach is computationally expensive.

(Kirar et al., 2021) proposed a method for computer-based glaucoma identification using fine sub-band images (SBIs) based on (SS-QB-VMD) second-stage quasi-bivariate variational mode decomposition using fundus pictures. First, five SBIs are created from the preprocessed images using QB-VMD. A total of 150 photos from the Retinal database were used for the proposed technique RIM One dataset (70 glaucoma images and 80 non-glaucoma images). A public huge image collection has also been used to implement the suggested strategy. It has 705 images, of which 309 are of healthy persons and 396 are of glaucoma patients. This approach obtains accuracy from 150 and 705 photographs, respectively, of 92.67% and 92.06%.

Fundus images should be divided into groups for normal and glaucoma using a least square support vector machine classifier, according to (Khan et al., 2022).The proposed method is examined using 455 RIM-One pictures from the MIAG (Medical Image Analysis Group). There are 255 fundus photos that fit into the normal category and 200 that fit into the glaucoma category. A maximum classification accuracy of roughly 91.22% is provided by the suggested method.

Using a dataset of 5716 images from Asian and Caucasian populations, (Ramesh et al., 2021) developed a deep learning system with a binary classifier for glaucoma screening. According to the findings, pictures with detectable glaucoma had an AUC of 94%.A researcher developed an automated glaucoma screening framework that uses an SVM classifier and Alexnet model to improve classification accuracy. This study used the datasets was compiled from a number of publicly available datasets, including fundus photos taken at Little Flower Hospital and Research Centre and HRF, Origa, Drishti, and others.

Table 1: Summary of Related Work

	Method	Dataset name	Dataset classes/Images	Accuracy
{Kirar, 2018 #124}	DWT & LS-SVM / 10 FCV	RIM-One (30)	15 glaucoma and 15 Healthy images	88.3
{Diaz-Pinto, 2019 #125}	SS-DCGAN	RIM-ONE, HRF, ACRIMA, ORIGA-light, and DRISHTI-GS	86926 images	0.9017
{Agrawal, 2019 #3}	QB-VMD) approach	RIM-ONE data set	505 images	86.13%
{Guo, 2020 #115}	GBDT+ADASYN	ORIGA dataset	650 color fundus im ages	0.843,
{Serte, 2021 #120}	AlexNet+ResNet-50 + ResNet- 152	fundus images	1542 fundus images no glaucoma, early glaucoma and advanced glaucoma	0.88
{Ajitha, 2020 #53}	R-CNN ResNet-50	ORIGA, and DRASHTI-GS	751 images	92.5%
{Zedan, 2023 #126}	SS-QB-VMD & LS-SVM / 10 FCV	RIM-One (150)	80 non-glaucoma images and 70 glaucoma images	92
{Sunija, 2022 #78}	LS-SVM classifier	RIM-One of MIAG	455 images 200 glaucoma and 255 normal	91.22%
{Kirar, 2019 #66}	SoftMax classifier	HRF, Origa,Drishti, and Images from LF	1113 images	93.86%
{Khan, 2022 #58}	Deep learning	5716 images from Asian and Caucasian populations	5716 images	AUC of 94%
{Latif, 2023 #61}	ODGNet	ORIGA, HRF, DR-HAGIS, RIM-ONE and DRIONS-DB,	958 public retinal fundus 665 healthy images, 293 glaucomatous images)	95.75 ORIGA
{Al-Mahrooqi, 2022 #62}	*(GARDNet)*	EyePACS AIROGS RIM-ONE DL dataset	313 normal and 172 glaucomatous	0.9308
{Nawaz, 2022 #98}	(FRCNN)Fast Region-based Convolutional Neural Network	Diaretdb1, MESSIDOR, HRF datasets. ORIGA, and DR-HAGIS,	89 fundus samples 1200 images 40 images 45 images 650 data samples,	95%
{Zhao, 2021 #9}	MFPPNet CNN	Direct-CSU and public ORIGA,	421 fundus images.	0.905
{Singh, 2023 #93}	UNet++	ORIGA,	650 color fundus images	0.84
{Alghamdi, 2021 #31}	SSCNN-DAE	RIM-ONE and RIGA	455 retinal images 750 retinal fundus images	0.93
{Hemelings, 2023 #127}	DNN	fundus images	2643 image	AUC: 94%

The SoftMax classifier achieved a 93.86% accuracy rate. The labelled data used for training the model is a replica of this study. Large datasets are used by DL models to learn the features needed to make precise predictions. Retinal image annotation is expensive and time-consuming. The acceptance of the DL methods' black box approach by medical professionals is another difficulty.

3. Research Methodology

3.1. Strategy and Methodology for Disease classification

In this section I have presented my research approach for the complete research part to classify the glaucoma disease from the dataset. The Fig 3-1 shows the overall proposed system and research strategies.

Figure 1: Strategy Diagram Representation

In this section I have presented my research approach for the complete research part to classify the glaucoma disease from the dataset. The Fig 1 shows the overall proposed system and research strategies. Since the project's goal is to implementing a classifier, this goal will be accomplished by developing a program that uses multi-level deep learning to localize and categorize glaucoma illness. This project involves developing and implementing a program in addition to being technical to differentiate different types of disorders and defects with the available technologies; research—it looks at the knowledge and applications already in use in this area of study. As a result, the approach used will be the one referred to as "Design and Creation". Utilizing Fig in an iterative process as part of the Design and Creation technique entails keeping in mind that each stage must be completed before continuing.

3.2. Development Tool for Research Implementation

To design and develop an effective framework, it is critical to use the best tool. Several different programming paradigms are supported by the high-level, general-purpose language Python including structural, functional programming and, object-oriented (OOP), It is intended to be a straightforwardly accessible language (Passerini & Lombardi, 2020). To design a solution centered on deep learning in the early days, it was critical to have competence in C++ and CUDA, which few individuals possessed. At the moment, the fundamental Python scripting capabilities are sufficient to conduct advanced deep learning investigations (Perkins, 2017). Thus, Python is the language of choice for programmers worldwide when it comes to implementing a deep learning-based solution. Python language performs well due
to its integration of specialized libraries for each type of task and functional programming.

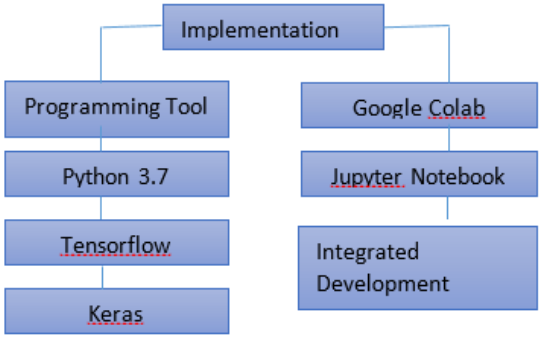

Figure 2: Implementation of the project

3.3. Dataset

The effectiveness of deep learning techniques depends on a valid and appropriate dataset being available. This research is using the following dataset. Generated eye dataset for glaucoma detection dataset can be downloaded from Kaggle's website. The corresponding website and unique ID for the dataset is: (https://www.kaggle.com/datasets/hindsaud/datasets-higancnn-glaucoma-detection). We take HRF dataset from this dataset.The HRF dataset has a total of 6000 images.

The HRF dataset is available in three main folders, training, testing, and validation. It has 2 classes - one is normal and other is glaucoma disease. After splitting the dataset, there are 4200 samples in the train set, 900 samples in the test set, and 900 samples in the validation set.

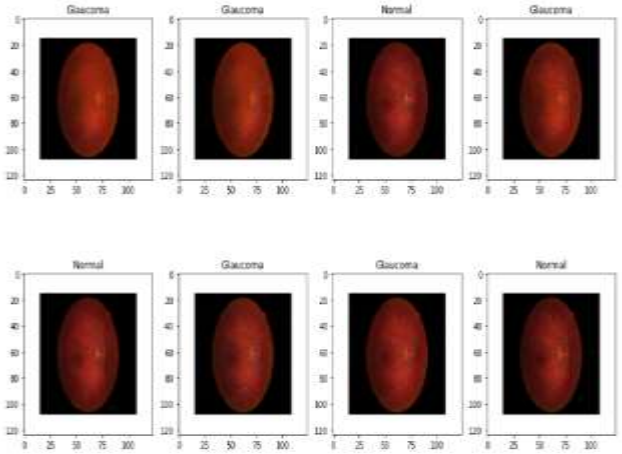

Figure 3: Dataset images

Table 1: Summary of the HRF dataset

Class Labels	Training	Testing	Validation
Normal	2100	450	450
Glaucoma	2100	450	450
Total	4200	900	900

3.4. Proposed methodology

3.4.1. Preprocessing

Pre-processing procedures include those that best prepare or enable the image for subsequent processing. Preprocessing is used to enhance the quality and contrast of the retinal fundus image by removing noise and fluctuation. The preprocessing phase can be used for image normalization and non-uniform intensity correction in addition to contrast enhancement and noise reduction to remove artefacts and improve the accuracy of the subsequent processing steps. The HRF dataset's input images are all preprocessed in order to produce stronger features and more consistent classification results.

3.4.2. Image resizing

Image's physical size changes as a result of resizing. Resizing to similar degrees preserves the data, but if pixels need to be combined to create a new size, it might lose some of the detail. Numpy will convert the image dataset into an array. The asarray () method is used to transform NumPy arrays from PIL images. The original dataset contains 128 ×128 versions of each image. The dataset has been scaled down to 124 ×124. The model performance will be drastically reduced, and the processing time will be sped up.

3.4.3. Data labeling

The process of giving unprocessed data—such as pictures, videos, text, and audio—tags or labels is known as data labelling. When an object class is identified in data without a tag, these tags help a machine learning model identify it. They also describe the object class to which the data belongs. It has 2 classes - one is normal and other is glaucoma disease. Create labels by Glaucoma and Normal. Normal labeled by zeros and glaucoma labeled by ones. After splitting the dataset, 900 samples make up the test set, 4200

samples make up the train set, and 900 samples make up the validation set. In our study, we use 70% of the dataset's photos for training, 15% for testing, and the remaining 15% for results validation.

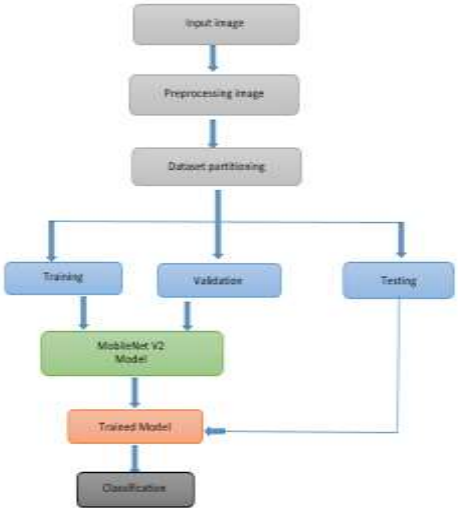

Figure 3: Proposed method flowchart

3.4.4. Data augmentation

Data augmentation is a strategy used to expand the amount of data by adding copies of previously existing data that have undergone significant updating or entirely new synthetic data that has been developed from previously existing data. The function "ImageDataGenerator" has been used from the Keras preprocessing library to apply the data augmentation. The image was rotated to a certain degree based on the parameters which indicated the 90 degree. The zooming augmentation was applied by zooming the image with 2% which was randomly selected from the image. The amount of photos we create from each input image is generated using a batch size of 64.

Table 3: Data augmentation operation

Augmentation	Range
Rotation	90˚
Zoom	2%
Horizontal flip	True
Vertical flip	True

3.5. Training, Validation and Testing

Training, testing, and validation components made up the HRF dataset. The training dataset was used to train the MobileNetV2 model, while the validation and test datasets were used to evaluate its performance. In order to accomplish this, we divided the dataset into three categories: testing, training, and validation, with corresponding weights of 70%, 15%, and 15%.The dataset shown in table 3-1 was used to train the MobileNetV2 model. 4200, 900, and 900 photos were used for the HRF dataset testing, training, and validation, respectively.

4. Data Analysis

4.1. Introduction

This chapter will give an overview over the achieved results of the proposed methodology. Confusion matrix of test data, ROC curve, model accuracy and model loss data are presented in figurative, tabular and graphical forms.

4.2. Training of MobileNetV2 for Classification

The Jupyter notebook in Google Colab (cloud computing) is implied for the proposed **MobileNetv2** model and the experimental environments are depicted in Table 4-1.It is trained for a number of iterations using Adam optimization and the binary cross entropy (Binary classification requires cross-entropy binary) loss function. The batch size of each epoch is constant (64) with some data augmentations. Table 4-1 shows the parameter configuration. Different evaluation parameters are set for the model's evaluation.

The ReLU (rectified linear unit) is a common activation function in artificial neural networks; we have indicated the regularized ReLU function as follows: $\boldsymbol{f(x) = max(0, x)}$

Here x is input, and f is ReLU.

The upper equation zeroes when using the ReLU function, which results in a network Sparsity that reduces parameter interdependence and reduces the occurrence of f(x) overfitting = max (0, x) g.

When sigmoid and tanh functions reproduce, their gradients in the saturation region are close to zero. The gradients are easy to disappear, leading to slower convergence and loss of information. In this case, the gradient of ReLU is a constant, helping to solve the deep network convergence problem. In the meantime, ReLU's unilateral function is more consistent with biological neuronal characteristics. CNN's with ReLU train with sigmoid units (Figure 4-1) or hyperbolic tangents more frequently than their equivalents (Yu et al., 2020).

4.3. Experiment Results and Discussion

On Google Colab, an experiment using the proposed MobileNetV2 architecture was run. Python, open-source Keras tools, and the Tensor-Flow platform were used to construct the MobileNetV2 technique. With a binary cross-entropy loss function and a default learning rate, it was trained using the Adam optimizer

The outcomes of the suggested MobileNetV2 model were concentrated on:

1. To distinguish the fundus images into normal or glaucoma.
2. By utilizing data augmentation approaches, assessed how well the specific MobileNetV2 model performed using the HRF dataset.
3. The outcomes were compared with state-of-the-art techniques.

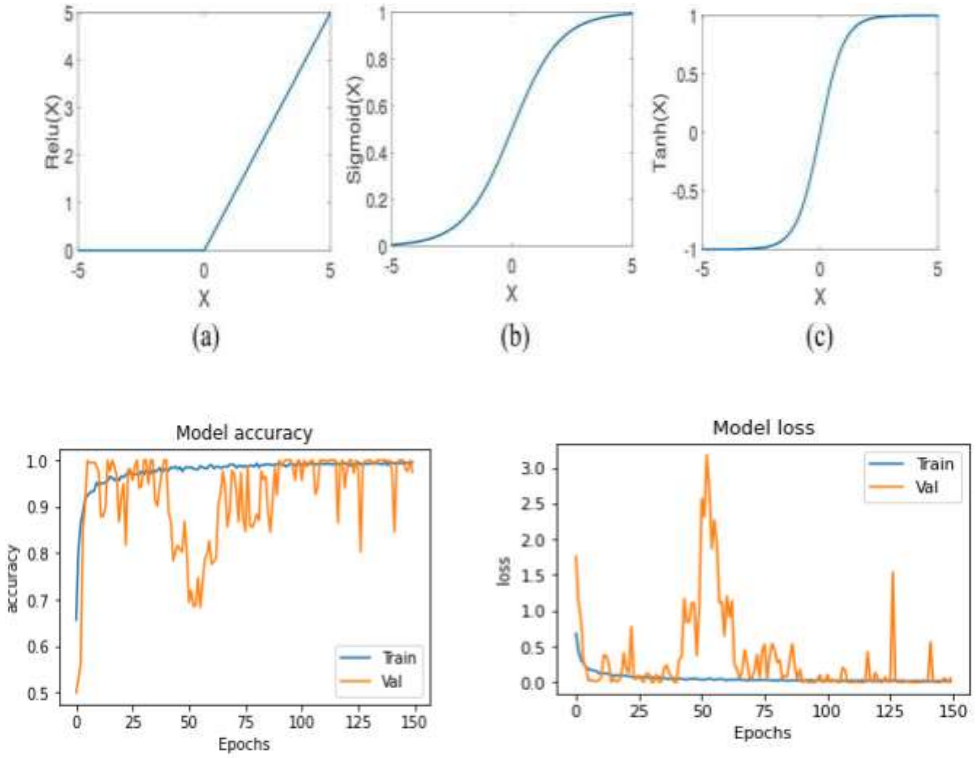

Figure 4-2: (a) Accuracy graph, and (b) loss graph of the proposed model

4.4. Proposed Model Performance on the HRF Dataset

Evaluation of the effectiveness of the recently deployed MobileNetV2 architecture was the experiment's main objective. The experiment employed the binary-cross entropy loss function, the Adam optimizer, 150 iterations, 64 batches, and the default alpha rate, as shown in Table 3. The experimental findings demonstrated that the introduced approach achieved 96% and 96% accuracy for normal and glaucoma, respectively. It also obtained an average accuracy of 96% on the HRF dataset, as shown in Table 4. The normal and glaucoma recall rates for the transfer learning model were 1.00 and 0.92, respectively. It achieved a precision of 0.93% for normal illnesses and 1.00% for glaucoma, respectively, with an F1-score of 0.96% for both disorders. The outcomes showed that using data augmentation techniques in the training set improved the classification scores produced by the suggested method on the HRF dataset.

Table 4: Classification accuracy, recall, precision and F1-score of presented MobileNetV2 Model on HRF dataset

Performance Measure	Normal	Glaucoma	Average Accuracy
Accuracy	0.98	0.98	0.97
Recall	1.00	0.92	0.96
F1-Score	0.96	0.96	0.96
Precision	0.93	1.00	0.955

5. Discussion

5.1. Conclusion and future work

Glaucoma is an irreversible disorder that results in intraocular hypertension because the drainage pathway between the iris and cornea is closed and there is an increase in aqueous fluid. Damage to the optic nerve head, which transmits visual information from our eyes to the brain, leads to vision field loss and eventually blindness. Because it is challenging to identify in its early stages, glaucoma is known as the stealth thief of eyesight. Ophthalmologists frequently utilize the Cup to Disc Ratio, or CDR measure, to diagnose glaucoma. The CDR parameters are still calculated manually, usually by skilled physicians using pricy and specialized equipment. In addition to the possibility of human error, glaucoma detection is an expensive and time-consuming process that also depends on the availability of resources (experienced ophthalmologists and expensive instruments). This work proposes a novel deep transfer learning model for classifying glaucoma using MobileNetV2. A framework called MobileNetV2 optimizes memory and execution speed utilization at the lowest possible cost in relation to the error. Low memory consumption is another desirable feature, and high execution speed greatly simplifies parameter customization and experimentation. In the future, we might train the model more to increase its accuracy. The proposed model can be trained on different datasets in future.

References

Ajitha, S., & Judy, M. (2020). Faster R-CNN classification for the recognition of glaucoma. Journal of Physics: Conference Series,

Alghamdi, M., & Abdel-Mottaleb, M. (2021). A comparative study of deep learning models for diagnosing glaucoma from fundus images. *IEEE Access*, *9*, 23894-23906.

Ansari, E., Pavicic-Astalos, J., Ayan, F., King, A. J., Kinsella, M., Ng, E., Nita, A., & Group, V. (2021). Treatment of open-angle glaucoma and ocular hypertension with preservative-free tafluprost/timolol fixed-dose combination therapy: UK and Ireland results from the VISIONARY Study. *Advances in therapy*, *38*(6), 2990-3002.

Arbeiter, D., Reske, T., Teske, M., Bajer, D., Senz, V., Schmitz, K.-P., Grabow, N., & Oschatz, S. (2021). Influence of drug incorporation on the physico-chemical properties of poly (L-lactide) implant coating matrices—A systematic study. *Polymers*, *13*(2), 292.

Camara, J., Neto, A., Pires, I. M., Villasana, M. V., Zdravevski, E., & Cunha, A. (2022). Literature review on artificial intelligence methods for glaucoma screening, segmentation, and classification. *Journal of Imaging*, *8*(2), 19.

Cvenkel, B., & Kolko, M. (2020). Current medical therapy and future trends in the management of glaucoma treatment. *Journal of Ophthalmology*, *2020*.

Devecioglu, O. C., Malik, J., Ince, T., Kiranyaz, S., Atalay, E., & Gabbouj, M. (2021). Real-time glaucoma detection from digital fundus images using self-onns. *IEEE Access*, *9*, 140031-140041.

Fu'adah, Y. N., Sa'idah, S., Wijayanto, I., Ibrahim, N., Rizal, S., & Magdalena, R. (2021). Computer Aided Diagnosis for Early Detection of Glaucoma Using Convolutional Neural Network (CNN). Proceedings of the 1st International Conference on Electronics, Biomedical Engineering, and Health Informatics: ICEBEHI 2020, 8-9 October, Surabaya, Indonesia,

Gharahkhani, P., Jorgenson, E., Hysi, P., Khawaja, A. P., Pendergrass, S., Han, X., Ong, J. S., Hewitt, A. W., Segre, A., & Igo Jr, R. P. (2020). A large cross-ancestry meta-analysis of genome-wide association studies identifies 69 novel risk loci for primary open-angle glaucoma and includes a genetic link with Alzheimer's disease. *BioRxiv*, 2020.2001. 2030.927822.

Guo, F., Li, W., Tang, J., Zou, B., & Fan, Z. (2020). Automated glaucoma screening method based on image segmentation and feature extraction. *Medical & Biological Engineering & Computing*, *58*, 2567-2586.

Hervella, Á. S., Rouco, J., Novo, J., & Ortega, M. (2022). End-to-end multi-task learning for simultaneous optic disc and cup segmentation and glaucoma classification in eye fundus images. *Applied Soft Computing*, *116*, 108347.

Islam, M. T., Mashfu, S. T., Faisal, A., Siam, S. C., Naheen, I. T., & Khan, R. (2021). Deep learning-based glaucoma detection with cropped optic cup and disc and blood vessel segmentation. *IEEE Access*, *10*, 2828-2841.

Kanse, S. S., & Yadav, D. M. (2019). Retinal fundus image for glaucoma detection: A review and study. *Journal of Intelligent Systems*, *28*(1), 43-56.

Khan, S. I., Choubey, S. B., Choubey, A., Bhatt, A., Naishadhkumar, P. V., & Basha, M. M. (2022). Automated glaucoma detection from fundus images using wavelet-based denoising and machine learning. *Concurrent Engineering*, *30*(1), 103-115.

Khatib, T. Z., & Martin, K. R. (2020). Neuroprotection in glaucoma: towards clinical trials and precision medicine. *Current Eye Research*, *45*(3), 327-338.

Kirar, B. S., Reddy, G. R. S., & Agrawal, D. K. (2021). Glaucoma Detection Using SS-QB-VMD-Based Fine Sub-Band Images from Fundus Images. *IETE Journal of Research*, 1-12.

Latif, J., Tu, S., Xiao, C., Ur Rehman, S., Imran, A., & Latif, Y. (2022). ODGNet: a deep learning model for automated optic disc localization and glaucoma classification using fundus images. *SN Applied Sciences*, *4*(4), 98.

Nawaz, M., Nazir, T., Javed, A., Tariq, U., Yong, H.-S., Khan, M. A., & Cha, J. (2022). An efficient deep learning approach to automatic glaucoma detection using optic disc and optic cup localization. *Sensors*, *22*(2), 434.

Nayak, D. R., Das, D., Majhi, B., Bhandary, S. V., & Acharya, U. R. (2021). ECNet: An evolutionary convolutional network for automated glaucoma detection using fundus images. *Biomedical Signal Processing and Control*, *67*, 102559.

Neto, A., Camara, J., & Cunha, A. (2022). Evaluations of deep learning approaches for glaucoma screening using retinal images from mobile device. *Sensors*, *22*(4), 1449.

Nguyen, T. X., Ran, A. R., Hu, X., Yang, D., Jiang, M., Dou, Q., & Cheung, C. Y. (2022). Federated learning in ocular imaging: current progress and future direction. *Diagnostics*, *12*(11), 2835.

O'bryhim, B. E., Samara, A., Chen, L., Hershey, T., Tychsen, L., & Hoekel, J. (2022). Longitudinal Changes in Vision and Retinal Morphology in Wolfram Syndrome. *American journal of ophthalmology*, *243*, 10-18.

Passerini, N., & Lombardi, C. (2020). Postponing the Concept of Class When Introducing OOP. Proceedings of the 2020 ACM Conference on Innovation and Technology in Computer Science Education,

Perkins, H. (2017). CUDA-on-CL: a compiler and runtime for running NVIDIA® CUDA™ C++ 11 applications on OpenCL™ 1.2 Devices. Proceedings of the 5th International Workshop on OpenCL,

Ramesh, P. V., Parthasarathi, S., & John, R. K. (2021). An exploratory study of compliance to anti-glaucoma medications among literate primary glaucoma patients at an urban tertiary eye care center in South India. *Indian journal of ophthalmology*, *69*(6), 1418.

Robbins, C. C., Anjum, S., Alwreikat, A. M., Cooper, M. L., Cotran, P. R., Roh, S., & Ramsey, D. J. (2021). An initiative to improve follow-up of patients with glaucoma. *Ophthalmology Science*, *1*(4), 100059.

Saxena, A., Vyas, A., Parashar, L., & Singh, U. (2020). A glaucoma detection using convolutional neural network. 2020 international conference on electronics and sustainable communication systems (ICESC),

Serte, S., & Serener, A. (2021). Graph-based saliency and ensembles of convolutional neural networks for glaucoma detection. *IET Image Processing*, *15*(3), 797-804.

Shoba, S. G., & Therese, A. B. (2020). Detection of glaucoma disease in fundus images based on morphological operation and finite element method. *Biomedical Signal Processing and Control*, *62*, 101986.

Singh, L. K., Khanna, M., Thawkar, S., & Singh, R. (2023). Nature-inspired computing and machine learning based classification approach for glaucoma in retinal fundus images. *Multimedia Tools and Applications*, 1-49.

Yu, Y., Adu, K., Tashi, N., Anokye, P., Wang, X., & Ayidzoe, M. A. J. I. A. (2020). Rmaf: Relu-memristor-like activation function for deep learning. *8*, 72727-72741.

Zhao, W., Lv, X., Wu, G., Zhou, X., Tian, H., Qu, X., Sun, H., He, Y., Zhang, Y., & Wang, C. (2021). Glaucoma is not associated with Alzheimer's disease or dementia: a meta-analysis of cohort studies. *Frontiers in Medicine*, *8*, 688551.